ELSEVIER

Journal of Organometallic Chemistry 536–537 (1997) 139–147

Journal of Organometallic Chemistry

Dihydrogen addition to $(P^iPr_3)_2OsX_nH_{4-n}$ [1]

Roger Kuhlman [a], Dmitry G. Gusev [a], Igor L. Eremenko [b], Heinz Berke [b], John C. Huffman [a,*], Kenneth G. Caulton [a]

[a] *Department of Chemistry and Molecular Structure Center, Indiana University, Bloomington, IN 47405-4001, USA*
[b] *Institute of Inorganic Chemistry, University of Zürich, Winterthurerstr. 190, Zürich, Switzerland*

Received 29 May 1996; accepted 14 November 1996

Abstract

Reaction of H_2 with $L_2Os(X)(Y)(H)_2$ ($L = P^iPr_3$; X, Y = Cl, Br, I) slowly (minutes) gives a 1:1 'adduct'. The X-ray structure of $L_2OsH_4Br_2$ shows, like the chloride analog, a substantial change in geometry upon reaction with H_2, to give a heavy atom OsX_2L_2 skeleton of C_{2v} geometry, with *cis* halides and *trans* phosphines. Attempts are made to distinguish between $Os(H)_4$, $Os(H_2)_2$ and $Os(H)_2(H_2)$ structures using J_{HD} and T_{1min} criteria. Study of $L_2OsX_nH_{4-n}$ species shows no monotonic trend in the $\Delta G^{\ddagger}$ for H_2 loss, being higher for both $n = 0$ and $n = 2$ than for $n = 1$. Studied as a function of X (= Cl, Br, I), H_2 binding to $L_2Os(H)_2X_2$ is favored enthalpically but disfavored entropically for the larger, least electronegative halide. The X-ray structure of L_2OsDCl_3 shows this unsaturated species to have significant angular distortions from octahedral geometry, consistent with its diamagnetic character. © 1997 Elsevier Science S.A.

Keywords: Osmium; Hydride addition; Crystal structure; π-bonding; Halogen; Hydrogen

1. Introduction

Unsaturated transition metal hydrido halide complexes offer the opportunity to probe the nature of the metal halide bond. In recent years, we have explored the idea that this bond, and those involving other π-donor groups like OR, SR, NR_2, PR_2, can have multiple bond character

$$\underset{\mathbf{A}}{M-\ddot{X}} \leftrightarrow \underset{\mathbf{B}}{M\overset{\leftarrow}{-}X}$$

and that this can diminish the ground state 'unsaturation' (low energy empty orbital, or Lewis acid character) of such a molecule. At the same time, such π-donation (**B**) can be displaced by an incoming nucleophile, thereby leaving unaltered the concept of unsaturation in an operational sense. It has also been pointed out [1] that when a potential π-donor ligand X has its lone pair localized on X in an 18-electron complex (e.g. $RuClH(PR_3)_4$), it creates a four-electron repulsion (destabilization) which makes the metal more reducing, and more Brønsted basic. We are interested in establishing (semi)quantitative evidence (e.g. thermodynamic) on the donor ability of halide ligands. For this purpose, it is best to use a carbonyl-free metal complex, since a CO ligand diminishes this four-electron destabilization by a 'push/pull' interaction [2]. We report here one test study, using H_2 as the probe Lewis base towards various $L_2OsCl_nH_{4-n}$ species.

2. Results

2.1. Reactions of $L_2OsX_nH_{4-n}$ with H_2

In order to test the importance of π-donating ligands, we compared the reactivity of these $L_2OsCl_nH_{4-n}$ complexes ($L = P^iPr_3$) toward an added ligand. We tested their reactivity with H_2, because it is (a) generally weakly binding, and thus most likely to discriminate most clearly, (b) able to either bind intact or to oxidatively add, and (c) easily studied spectroscopically. We hoped first to survey the reactivity according to number of halide ligands, and then investigate the more subtle influences within a structure type by varying the type of X ligand.

* Corresponding author.

[1] Dedicated to Yuri Struchkov, for his extraordinarily broad interests in chemistry, for the strength of his opinions, and for his willingness to be helpful.

PII S0022-328X(96)06914-8

2.2. Effect of the number of X ligands

This initial survey of reactivity is discussed only in terms of chloride ligand, for the sake of simplicity, but the statements generally hold for the other halides. There is a very clear trend that the tendency for H_2 coordination to $L_2OsCl_nH_{4-n}$ is diminished by incorporation of π-donating ligands (increasing n). When $n = 0$, H_2 binding is highly favored, and the 16-electron complex 'L_2OsH_4' has not been isolated or directly observed. It can neither be synthesized, nor even trapped by some ligand: L_2OsH_6 does not react with MeCN or CO (days at room temperature), because no 16-electron species is formed to permit a ligand substitution. Moreover, there is no dihydrogen ligand in L_2OsH_6. The shortest HH separation in the neutron structure of $(P^iPr_2Ph)_2OsH_6$ was found to be 1.650(6) Å [3]. The complex with $L = P^iPr_3$ presumably has a classical structure as well, since we have measured it to have a long T_{1min} (119 ms at 300 MHz).

When $n = 1$ and X = halide, H_2 binds as a virtually intact dihydrogen ligand, forming complexes $L_2OsH_3X(H_2)$ [4]. Binding of H_2 is essentially quantitative under one atmosphere of H_2 at room temperature. However, the H_2 ligand is easily lost when $L_2OsH_3Cl(H_2)$ is exposed to vacuum. Spin-saturation transfer indicates an exchange of free and coordinated H_2 at −20 °C [5]. When X = Cl, the H_2 ligand has a H–H distance of 0.95 Å, based on our measured value of T_{1min} [6].

Binding of H_2 is less thermodynamically favorable for $L_2OsH_2Cl_2$ ($n = 2$) than for L_2OsH_3Cl ($n = 1$). At room temperature under excess H_2, this 16-electron complex is still observed, along with its H_2 adduct, in about a 1:1 ratio. Based on T_{1min} measurements (see Scheme 2 and discussion below), the H–H distance can be 1.3–1.4 Å if an $L_2OsH_2Cl_2(H_2)$ formulation is assumed, indicating a strongly activated ('stretched') dihydrogen ligand. [Assuming the $L_2OsH_2Cl_2(H_2)$ formulation, and taking $R^* = 8.4\,s^{-1}$ from the value we measure in L_2OsH_6; R^* is the relaxation contribution from all nuclei except the other H in an H_2 ligand.] Thus, even though there is more backbonding to H_2 in $L_2OsH_2Cl_2(H_2)$, H_2 binding to $L_2OsH_2Cl_2$ is less thermodynamically favorable than it is to L_2OsH_3Cl. This counterintuitive result can be explained by considering both reactants and products in the two reaction free energy diagrams (Scheme 1). While more Os–H bonding is lost when H_2 dissociates from $L_2OsH_2Cl_2(H_2)$, more Cl–Os π-bonding is also created to compensate for that loss.

Exchange with free H_2 is much faster for $L_2OsH_3Cl(H_2)$ than for $L_2OsH_2Cl_2(H_2)$. For the monochloride complex, spin saturation transfer (timescale of seconds) demonstrates the exchange, whereas several minutes are required for the dichloride complex

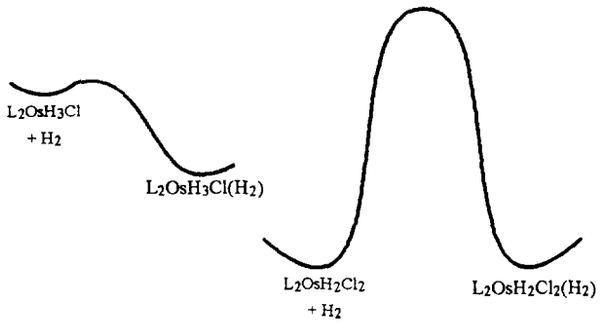

Scheme 1.

to establish equilibrium. The primary reason for this large kinetic barrier in the dichloride complex is presumably the significant changes in the heavy-atom positions between the unsaturated complex (P–Os–P angle 112°) [7] and the 18-electron complex (P–Os–P angle 176.9(1)°) [5]. In sharp contrast, the phosphine ligands are in *trans* positions in both L_2OsH_3Cl and $L_2OsH_3Cl(H_2)$, and require almost no motion upon H_2 coordination. In summary, H_2 binding to L_2OsH_3Cl is looser, faster, and yet more thermodynamically favorable than it is to $L_2OsH_2Cl_2$ (Scheme 1).

L_2OsHCl_3, in the presence of 1 atm H_2 in CD_2Cl_2 or in Freon, shows no change in its ^1H or $^{31}P\{^1H\}$ NMR chemical shifts at 25 °C. However, in the temperature range −10 to −135 °C in Freons, the ^{31}P chemical shift moves progressively from −98.9 to −89.8 ppm. This is consistent with a coalesced resonance of the two complexes shown in Eq. (1), where $L_2OsH_3Cl_3$ has a chemical shift upfield from that of L_2OsHCl_3. The binding of H_2 to L_2OsHCl_3 is clearly weaker than that to the di- and monohalide analogs.

$$L_2OsHCl_3 + H_2 \leftrightharpoons L_2OsH_3Cl_3 \quad (1)$$

The observations of H_2 coordination to $L_2OsCl_nH_{4-n}$ as a function of n are summarized in Table 1. The clearest trend is in $-\Delta G°$ of H_2 binding. Thermodynamically, H_2 coordination is disfavored by chloride ligands with respect to hydride ligands. The most likely explanation for the trend is the degree of X → M π-bonding which both stabilizes 16-electron complexes, and destabilizes 18-electron complexes [1].

2.3. Variation of the X ligand

We sought to investigate the more subtle influences of variation of the X ligand on H_2 binding kinetics and

Table 1
Summary of H_2 binding for $L_2OsCl_nH_{4-n}$ complexes

	Shortest HH distance	$-\Delta G°$ (H_2 binding)	$\Delta G^{\ddagger}$ (H_2 loss)
$n = 0$	1.65	very high	very high
$n = 1$	0.95	high	low
$n = 2$	1.25	low	high

thermodynamics for $n = 1$ and 2 and X = Cl, Br, I and alkoxide. In no case was there any evidence for a different structure type upon changing X (in either 16- or 18-electron complexes), although some distances and angles may change slightly.

2.4. H_2 Addition to L_2OsH_3X

All three halide complexes bind H_2 quite proficiently [6]. The H_2 ligand is believed to occupy a position *cis* to the halide, with the H–H axis aligned with the P–P vector in a pentagonal bipyramidal geometry. According to T_{1min} measurements [6] in methylcyclohexane-d_{14}, the H–H distance follows the order X = Cl (0.95 Å) < Br (1.05 Å) < I (1.13 Å). This trend is consistent with the most Os–H_2 backbonding occuring in the iodide complex, as would be predicted by the trend in halide electronegativity. Addition of H_2 to $L_2OsH_3(OR)$ was not investigated due to elimination of ROH and formation of L_2OsH_6.

2.5. H_2 Addition to $L_2OsH_2X_2$

These dihalide complexes [7,8] all slowly coordinate H_2, as has been reported for the dichloride complex [5]. In the previous communication on $OsH_4Cl_2(P^iPr_3)_2$, the ^1H NMR spectrum at −105 °C revealed two broad lines, which was interpreted in terms of (1) a mixture of isomers and (2) intramolecular fluxionality within each isomer which had not yet been halted. More extensive low-temperature decoalescence in the hydride region now more clearly reveals an equilibrium between the two tautomers. Shown in Fig. 1 are variable-temperature hydride region ^1H NMR spectra for $L_2OsCl_2H_4$, and Fig. 2 shows spectra for $L_2OsCl_2H_xD_{4-x}$. The signals for the partially-deuterated sample are better resolved, probably because of slower site exchange due to a kinetic isotope effect and/or removal of spin–spin relaxation mechanisms. Decoalescence of resonances from adjacent hydrides in this manner is rather unusual, and requires very low temperatures, only accessible via solvents like the Freon mixture employed ($CDFCl_2/CDF_2Cl$). Very similar spectroscopic behavior is observed for the other halide complexes. These spectra seem to indicate the configuration with one H_2 ligand (decoalescence to two signals) as predominant. The structure of the minor isomer (single hydride chemical shift at −150 °C) remains unknown. Because of this uncertainty in structural assignments, the trends in T_{1min} and J_{HD} (Table 2) must be interpreted with caution. There appears to be the most dihydrogen-ligand character in the dichloride complex, indicating shorter H–H distances in the equilibrium.

The comparative binding equilibria of H_2 to the $L_2Os(H)_2XY$ complexes were measured by exposing mixtures of the complexes to H_2 in $CDCl_3$ (i.e. by 'internal competition'). The mixtures were allowed several days to come to equilibrium at +21 °C, and several weeks at −21 °C. The relative equilibrium binding constants were then determined by measuring the ratio $R1$ (Eq. (2)) by integration of ^{31}P NMR signals, and the ratio $R2$ (Eq. (3)) by integration of ^1H NMR hydride signals. (The ^1H NMR signals of $L_2OsX_2H_4$ are not well resolved, nor are the ^{31}P NMR signals for

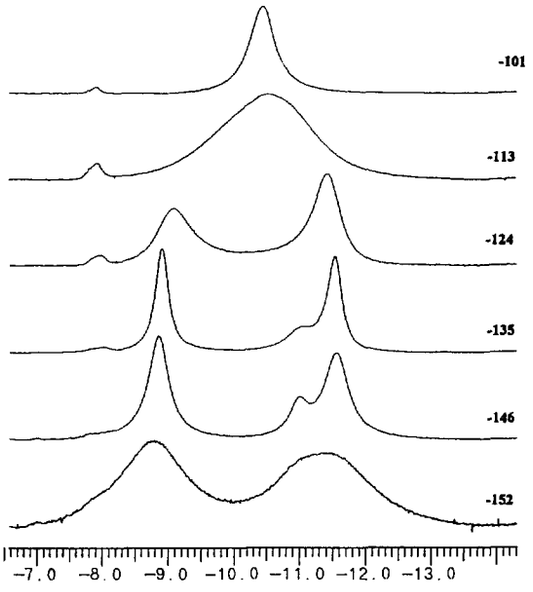

Fig. 1. Hydride region ^1H NMR spectrum of $L_2OsCl_2H_4$ in $CDFCl_2/CDF_2Cl$ at 300 MHz. Temperatures are given in degrees Celsius.

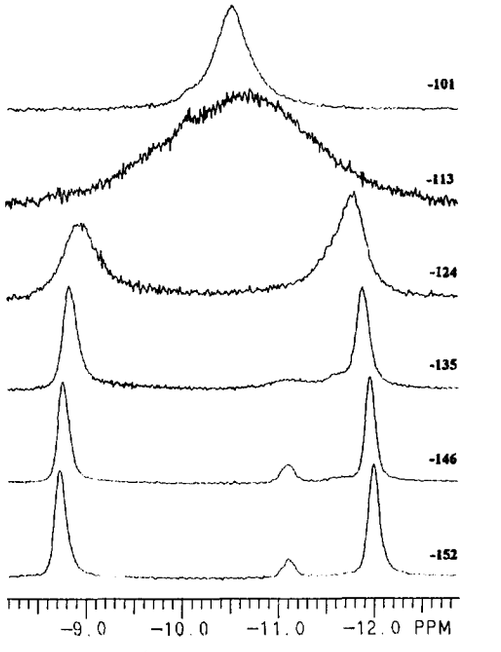

Fig. 2. Hydride region ^1H NMR spectrum of $L_2OsCl_2H_xD_{4-x}$ in $CDFCl_2/CDF_2Cl$ at 300 MHz. Temperatures are given in degrees Celsius.

Table 2
Structural and thermodynamic data for complexes $L_2OsX_2H_4$

	$L_2OsCl_2H_4$	$L_2OsClIH_4$	$L_2OsBrIH_4$	$L_2OsBr_2H_4$	$L_2OsI_2H_4$
T_{1min} (ms) [a]	39(1)	—	—	41(1)	46(1)
av. J_{HD} (Hz)	4.5	—	—	4.0	3.5
$\Delta\Delta G°$ (21 °C) (cal mol^{-1})	−310	−570	−400	−460	0
$\Delta\Delta G°$ (−21 °C) (cal mol^{-1})	−48	−370	−270	−350	0
$\Delta\Delta H°$ (kcal mol^{-1})	+1.5	+0.8	+0.5	+0.3	0
$\Delta\Delta S°$ (cal mol^{-1} K^{-1})	+6.2	+4.7	+3.1	+2.6	0

[a] At −70 °C for the coalesced signal.

$L_2OsX_2H_2$ complexes.) The ratio of equilibrium constants K_x/K_y (K defined in Eq. (4)) is simply $R1 \times R2$. The concentration of H_2 is cancelled out of the equation, since it is rigorously the same for K_x and K_y (same NMR tube). From K_x/K_y, $\Delta\Delta G°$ is easily calculated, $\Delta\Delta H°$ and $\Delta\Delta S°$ are then calculated from the values of $\Delta\Delta G°$ at the two different temperatures. The mixed dihalide complexes (which are generated upon mixing of the homodihalides) were analyzed in the same manner. Signals in the ^1H spectra of the mixed solution X = Cl/Y = Br were too broad for accurate integration, so data for L_2OsH_2ClBr are unavailable. These thermodynamic measurements are summarized in Table 2 and are scaled with reference to X = Y = I (chosen as zero).

$$R1 = \frac{[L_2OsX_2H_4]}{[L_2OsY_2H_4]} \quad (2)$$

$$R2 = \frac{[L_2OsY_2H_2]}{[L_2OsX_2H_2]} \quad (3)$$

$$K_x = \frac{[L_2OsX_2H_4]}{[L_2OsX_2H_2][H_2]} \quad (4)$$

At either temperature, the relative binding free energies follow the trend [Os]Br_2 (strongest binding) > [Os]Cl_2 > [Os]I_2 (weakest), which is a somewhat confusing trend. The trends in $\Delta H°$ and $\Delta S°$ are more easily analyzed. Enthalpically, H_2 binding follows the trend [Os]I_2 (best H_2 binder) > [Os]Br_2 > [Os]Cl_2 (worst). Many factors determine $\Delta H°$, including degree of Os–H_2 backbonding in the 18-electron complex, and X → M π-bonding in the 16-electron complex. The longer T_{1min} and smaller J_{HD} for $L_2OsI_2H_4$ indicate a greater degree of backbonding in this complex, in agreement with the direction of the trend. Additionally, there is some evidence for Cl to be a better π-donating ligand than I [2,9], which also supports the observed trend by destabilizing $L_2OsH_2I_2$ relative to $L_2OsH_2Cl_2$. Entropically, coordination of H_2 follows the order [Os]Cl_2 (most entropy-releasing) > [Os]Br_2 > [Os]I_2 (least). This trend is explained by steric factors. The H_2 adduct is most crowded for X = I. The general rule holds that H_2 binding to complexes with heavier halides is favored enthalpically ($\Delta H°$ is most negative for Os[I]$_2$) but disfavored entropically ($\Delta S°$ is least positive for Os[I]$_2$).

The bis-alkoxide complex $L_2Os(H)_2[OCH(CF_3)_2]_2$ [10] reacts very slowly with H_2 in toluene-d_8. After one hour of tumbling at room temperature under one atmosphere of H_2, $L_2Os(H)_2[OCH(CF_3)_2]_2$ is still the major phosphine-containing component of the reaction solution (approximately 80%), with the remainder being L_2OsH_6. After tumbling for days at room temperature, $L_2Os(H)_2[OCH(CF_3)_2]_2$ is completely consumed and the products observed are $L_2OsH_nD_{6-n}$ and $(CF_3)_2CHOH$. The presence of deuterium in L_2OsH_6 was recognized by the slight isotopic chemical shift dependence in the hydride signal. By integration of the hydride signal vs. ^{i}Pr resonances, the D-incorporation is estimated to be 38%. The reactions in Eqs. (5)–(8) could explain these observations. In this scheme, the reductive elimination of ROH generates a potent intermediate, capable of reacting with C–D bonds of toluene-d_8. In fact, the proposed intermediate in this scheme is L_2OsH_4, which should be extremely reactive due to its lack of π-donating ligands. As stated earlier, L_2OsH_6 has never been observed to lose H_2, so the reaction of Eq. (7) is expected to be quite exothermic.

$$L_2OsH_2(OR)_2 + H_2 \rightarrow L_2OsH_3(OR) + ROH(\text{slow}) \quad (5)$$

$$L_2OsH_3(OR) + H_2 \rightarrow L_2OsH_4 + ROH \quad (6)$$

$$L_2OsH_4 + n\text{toluene-}d_8 \rightarrow L_2OsD_nH_{4-n} + n\text{toluene-}d_7 \quad (7)$$

$$L_2OsD_nH_{4-n} + H_2 \rightarrow L_2OsD_nH_{6-n} \quad (8)$$

2.6. X-ray structure of $(P^iPr_3)_2OsBr_2H_4$

X-ray quality crystals of $L_2OsBr_2H_4$ were grown by storing a sealed tube containing $L_2OsH_2Br_2$ in CH_2Cl_2/CF_2Cl_2 (1:4) under H_2 for several days at −21 °C. The crystals are isomorphous with its chloride analog [5].

An ORTEP diagram is shown in Fig. 3, and bond distances and angles are given in Table 3. Hydrides

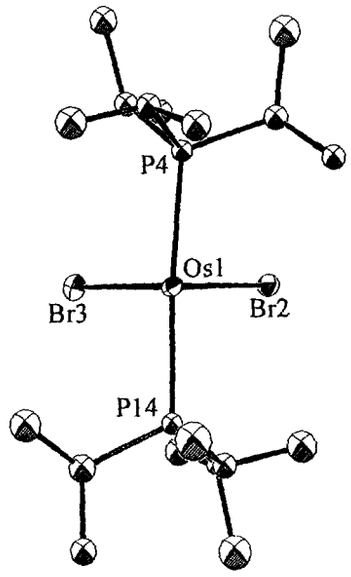

Fig. 3. ORTEP drawing of the non-hydrogen atoms of $(P^iPr_3)_2OsH_4Br_2$.

were not located crystallographically. The product of reaction with H_2 has a structure which differs greatly from that of its 16-electron precursor. $Os(H)_2Cl_2(P^iPr_3)_2$ has a non-octahedral structure with a P–Os–P angle of 112° and a Cl–Os–Cl angle of 83°. In $OsH_4Br_2(P^iPr_3)_2$, the two phosphines are almost exactly *trans* (P–Os–P angle 175.9(2)°), with usual Os–P distances (2.410(7) and 2.427(6) Å). The Br–Os–Br angle is only slightly less than 90° (88.9(1)°). The two Os–Br distances (2.580(3) and 2.591(3) Å) are essentially identical. While this leaves unanswered the question of whether they have identical ligands *trans* to them, the OsBr distances are so similar that it is unlikely that ligands as different as H and H_2 are *trans* to Br. On the other hand, a referee has observed that the Os–P distances agree well with previously determined Os(II)–P^iPr_3 distances, while they are longer than the 2.30–2.34 Å values in $OsH_4(PR_3)_3$ and $OsH_6(P^iPr_2Ph)_2$; this might suggest an $OsBr_2(H_2)_2L_2$ assignment.

Table 3
Selected bond distances (Å) and angles (°) for $OsH_4Br_2(P^iPr_3)_2$

Distances (Å)			
Os(1)	Br(2)	2.5796(25)	
Os(1)	Br(3)	2.591(3)	
Os(1)	P(4)	2.410(7)	
Os(1)	P(14)	2.427(6)	
Angles (°)			
Br(2)	Os(1)	Br(3)	88.90(9)
Br(2)	Os(1)	P(4)	87.05(16)
Br(2)	Os(1)	P(14)	89.80(16)
Br(3)	Os(1)	P(4)	94.02(16)
Br(3)	Os(1)	P(14)	88.60(16)
P(4)	Os(1)	P(14)	175.86(24)

Regarding the structure of $OsH_4X_2(P^iPr_3)_2$, certain conclusions follow from analysis of the combined low-temperature NMR and X-ray data available for X = Cl and Br. The major isomer of $OsH_4X_2(P^iPr_3)_2$ shows two resonances in the hydride region in solution. This observation and the equivalence of Os–X bonds in both solid-state structures suggest that the molecule possesses a plane of symmetry including the metal center and two phosphorus ligands. This plane bisects the X1–Os–X2 fragment. The osmium-bound hydrogens are therefore either all in the Os, X1, X2 plane or divided: two are in the Os, X1, X2 plane, while another pair is in the plane of Os, P, P.

A significant feature of the solid-state structures is that the two bulky P^iPr_3 are slightly bent toward the halides (∠P–Os–P = 176.9(1)° (Cl) [5] and 175.9(1)° (Br)). Related examples of $IrH(H_2)Cl_2(P^iPr_3)_2$ and $IrH_2Cl(P^tBu_2Ph)_2$, characterized by neutron diffraction [11], both show that the phosphines are bent away from the Cls in these molecules and toward the least sterically-demanding hydrogen ligands (∠P–Ir–P = 168.5(1)° and 172.3(1)° respectively). Apparently, the osmium complexes $OsH_4X_2(P^iPr_3)_2$ have two hydrogens in the Os, P, P plane and the molecular shape is then reminiscent of a dodecahedron where the trapezoids are P–H2–H3–P and H1–X1–X2–H4 (Scheme 2, left).

The structure of $IrH(H_2)Cl_2(P^iPr_3)_2$ provides additional relevant information. It shows a planar IrH_3Cl_2 fragment with the Cl–Ir–Cl angle of 87.0°, comparable to that in $OsH_4Cl_2(P^iPr_3)_2$, 88.7°. The two H–Ir–Cl angles are 78.0° and 83.3°; the former is smaller because of a possible attractive interaction between the *cis* halide and dihydrogen ligand. It is thus reasonable to

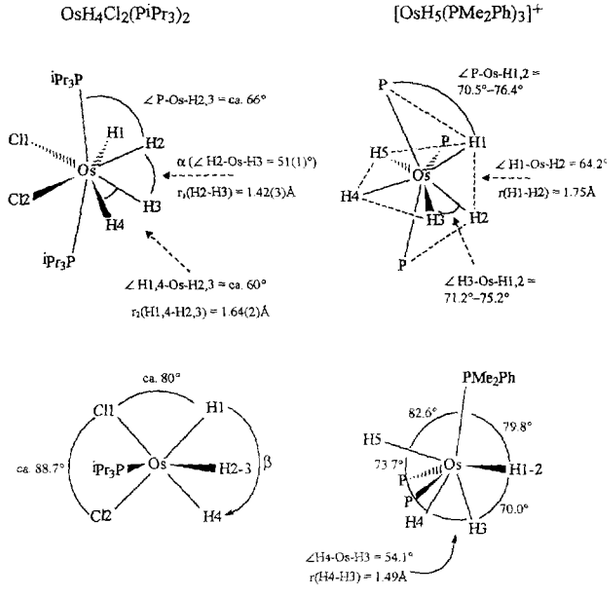

Scheme 2.

accept that two H1–Os–X1 angles in $OsH_4X_2(P^iPr_3)_2$ are about 80°.

Based on this symmetry, there are only two independent variables, angles $\alpha = \angle$H2–Os–H3 and $\beta = \angle$H1–Os–H4 (Scheme 2, left). An expression involving inter-hydride distances and the observed T_{1min} value (39 ms, 300 MHz) can be written as Eq. (9). This equation includes a dipole–dipole contribution of 4.5 s^{-1}, accounting for the interaction of the 'hydrides' with all P^iPr_3 protons.

$$0.5r_1^{-6} + 2r_2^{-6} = 0.164 \text{ where } r_1 = r(\text{H2–H3})$$
$$\text{and } r_2 = (\text{H(1 or 4)–H(2 or 3)}) \quad (9)$$

Assuming the Os–H distance is 1.65 Å [12], expressions can be written for r_1 and r_2 involving only the unknowns α and β. As discussed above, the smallest reasonable values for $\angle$H1–Os–Cl1 are in the range 70–80°. Thus, for $\beta = 113°$ (or 133°), α and r_1 are calculated to be 51° and 1.42 Å (or 46° and 1.29 Å) respectively. The observed T_{1min} value can thus be modelled with a structure (Scheme 2, left) somewhere between a dodecahedral tetrahydride and a pentagonal bipyramid with a pentagon comprised of 2 Cl, 2 H and 1 H_2 (i.e. that involving some close 'approach' or 'bonding' between H2 and H3). For comparison, the corresponding structural parameters [13] for $OsH_5(PMe_2Ph)_3^+$ are shown in Scheme 2, right. Short T_{1min} values of 50–43 ms (300 MHz) have also been measured for $OsH_5L_3^+$ where L = PPh_3 and P(p-tolyl)$_3$ [14].

2.7. $(^iPr_3P)_2OsHCl_3$

This molecule is the last member in the $L_2OsX_nH_{4-n}$ series. Synthetic transformation of $L_2OsH_2Cl_2$ to the trichloride member of the $L_2OsH_{4-n}Cl_n$ series is especially challenging. L_2OsDCl_3 was originally made by slow formation from a solution of $L_2OsD_2Cl_2$ under D_2 in CD_2Cl_2 in the presence of oxygen. We then sought a more systematic synthesis. Reaction of $L_2OsH_2Cl_2$ with one equivalent of N-chlorosuccinimide (NCS) in $CHCl_3$ yields a mixture of L_2OsHCl_3, unreacted $L_2OsH_2Cl_2$, and some unidentified product (perhaps L_2OsCl_4). Recrystallization from toluene and washing with H_2O (to remove succinimide) yields pure L_2OsHCl_3 in low yield, as a blue–green solid. This complex is soluble in polar solvents ($CDCl_3$, Freons, CD_2Cl_2), very poorly soluble in toluene, and insoluble in pentane or water. The complex is characterized by a doublet of doublets in the methyl region, indicating that the phosphines are not occupying *trans* sites. The hydride triplet does not decoalesce at −110 °C in CD_2Cl_2/toluene-d_8 (9:1), consistent with it being a monohydride complex with no second isomeric structure. The T_1 value of the hydride triplet of L_2OsHCl_3 in CD_2Cl_2 is 234(5) ms at −78 °C

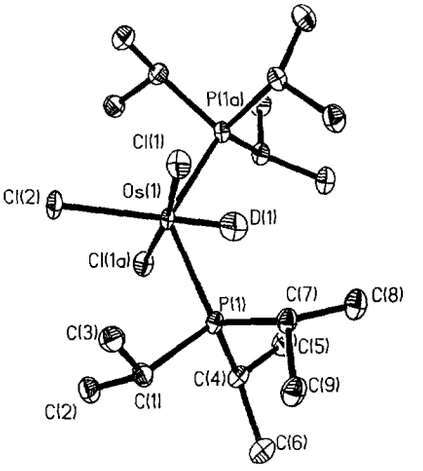

Fig. 4. ORTEP diagram of the non-hydrogen atoms of $(P^iPr_3)_2OsDCl_3$.

(this is near the minimum value), which is consistent with the monohydride formulation.

The structure of this complex has been determined by X-ray crystallography. An ORTEP diagram is shown in Fig. 4 and selected bond distances and angles in Table 4. The molecule has a crystallographically-imposed C_2 symmetry axis, so Os, Pl, Pla, Cl2, and D are all rigorously coplanar, as are atoms Os, Cl1, Cl1a, and Cl2. The most remarkable feature of the structure is the bent P–Os–P angle (126.4(2)°). The Cl1–Os–Cl2 angle is slightly less than 90° (86.0(1)°).

The structure of this complex reveals distortion from an octahedron analogous to that observed in $L_2Os(H)_3Cl$ [4]. Once again, two ligands distort away from their positions in an octahedron, raising one orbital of the former t_{2g} set. This maximization of σ-bonding can be effected by a range of different molecular deformations; the one observed is the one which also maximizes π-donation to Cl(2). The increased bonding between this chloride and the metal is reflected in the shorter Os–Cl2 bond length (2.311(4) Å) as compared to the Os–Cl1 bond lengths (2.391(4) Å).

Table 4
Bond distances and angles in $(P^iPr_3)_2OsDCl_3$

Distances (Å)			
Os1	Cl1	2.391(4)	
Os1	P1	2.308(4)	
Os1	Cl2	2.311(4)	
Os1	D1	1.60(2)	
Angles (°)			
Cl1	Os1	Cl2	86.0(1)
Cl1	Os1	P1	92.1(1)
Cl1	Os1	D1	94.0(1)
Cl2	Os1	D1	180.0
Cl1	Os1	Cl1A	172.0(2)
Cl1	Os1	P1A	91.5(1)
Cl2	Os1	P1	116.8(1)
P1	Os1	D1	63.2(1)

3. Conclusions

Hydrogen binding is favored thermodynamically by having fewer π-donating ligands, although kinetics of H_2 binding do not necessarily follow thermodynamic trends. The heavier halides favor H_2 coordination enthalpically, but disfavor it entropically in the $L_2OsH_2X_2$ system. Reductive elimination of ROH upon addition of H_2 to an unsaturated alkoxide complex leads to enhanced reactivity (H/D exchange with toluene-d_8).

4. Experimental

All reactions and manipulations were conducted using standard Schlenk and glovebox techniques. Non-aqueous solvents were dried and distilled under nitrogen or argon, and stored in air-tight solvent bulbs with Teflon closures. Deionized water was degassed prior to use. All NMR solvents were dried, vacuum-transferred, and stored in a glovebox. Complexes $(P^iPr_3)_2OsH_2X_2$ (X = Cl, Br, I) were synthesized according to published procedures [7,8]. Proton NMR spectra were obtained on a Varian XL-300 or a Bruker AM 500 spectrometer, while ^{31}P NMR spectra were recorded on a Nicolet 360 MHz instrument. All T_1 measurements were made at 300 MHz using the inversion–recovery method and standard Varian software. For additional details of determination of T_1 values and resulting H–H distances, see Refs. [6,8]. Chemical shifts are referenced to residual protio solvent peaks (^1H), or external H_3PO_4 (^{31}P). Temperatures were standardized according to the peak separation of CH_3OH; temperatures below $-100\,^\circ C$ require extrapolation and may be less reliable. Infrared spectra were recorded on a Nicolet 510P FT-IR spectrometer. The mixture of $CDFCl_2/CDF_2Cl$ was synthesized by the method of Siegel and Anet [15], and stored at $-20\,^\circ C$ in a glass bulb with Teflon closure.

4.1. Synthesis of $(P^iPr_3)_2OsHCl_3$

In a Schlenk flask, $L_2OsH_2Cl_2$ (0.140 g, 0.240 mmol) was combined with N-chlorosuccinimide (0.032 g, 0.240 mmol). The reactants were dissolved in $CHCl_3$ (15 ml). After stirring at room temperature for 2 days, the solvent was removed in vacuo, and the green solid was recrystallized from toluene. The product was washed with pentane (3 × 5 ml) and water (3 × 10 ml) and dried overnight in vacuo. Yield 0.030 g (0.049 mmol, 20%). ^1H NMR ($CDCl_3$, 20 °C): 3.50 (mult, 6H), 1.34 (dd, $J = 17.1$, 9.3, 36H), −24.32 (br, 1H). $^{31}P\{^1H\}$ NMR ($CDCl_3$, 20 °C): 107.2 ($\Delta\nu_{1/2} = 38$ Hz). Anal. Found: C, 35.82; H, 6.89; N, 0.08. Calc.: C, 34.94; H, 7.01%. The nitrogen present indicates succinimide impurity.

4.2. $(P^iPr_3)_2OsHBr_3$

An NMR tube was charged with $L_2OsH_2Br_2$ (0.010 g, 0.015 mmol) and N-bromosuccinimide (0.003 g, 0.017 mmol). The product L_2OsHBr_3 was pure by ^{31}P NMR, but contained several impurities visible by ^1H NMR. ^1H NMR ($CDCl_3$, 20 °C): 3.68 (mult, 6H), 1.36 (dd, $J = 15.6$, 5.4, 36H), −28 (br, 1H). $^{31}P\{^1H\}$ NMR ($CDCl_3$, 20 °C): 117.3 (s).

4.3. X-ray structure determination of $(P^iPr_3)_2OsDCl_3$

Prismatic green block-like crystals were grown by the following method: a brown solution of $(P^iPr_3)_2OsH_2Cl_2$ (0.050 g) in toluene-d_8/CD_2Cl_2 (ca. 1:9, 15 ml) under D_2 was slowly evaporated with access of air. Green prisms precipitated from the solution, and one with approximate dimensions $0.3 \times 0.2 \times 0.2\,mm^3$ was mounted on a glass fiber with 15 min epoxy resin. Accurate unit cell parameters (Table 5) were obtained by means of least-squares analysis of 34 reflections ($14^\circ \le 2\theta \le 22^\circ$). Intensity data were collected on a Siemens R3m/v diffractometer (24 °C, ω–2θ scans $4^\circ \ge 2\theta \ge 55^\circ$) (Table 5). An empirical absorption correction using ψ scans of 10 reflections was applied. The osmium atom was located by direct methods and all other non-hydrogen atoms were found in subsequent Fourier calculations. After anisotropic refinement of non-hydrogen atoms with H-atoms of P^iPr_3 ligands in geometrically-idealized positions, the deuteride atom was found in a successive Fourier map. Its position was refined isotropically. The final cycles of least-squares refinement gave $R = 0.043$, $R_w = 0.048$. The function minimized in the least-squares calculations was $\Sigma w(F_o$

Table 5
Crystallographic data for $(P^iPr_3)_2OsDCl_3$

Chemical formula	$C_{18}H_{43}Cl_3P_2Os$
Formula weight	618.0
Space group	$P2_12_12$ (No. 18)
a (Å)	8.986(3)
b (Å)	16.000(7)
c (Å)	8.603(3)
V (Å^3)	1236.9(8)
Z	2
ρ_{calc} (g cm^{-3})	1.659
T (°C)	24
λ (Mo Kα) (Å)	0.71073
μ (cm^{-1})	56.18
2θ range (°)	4–55
Min–max transmission coefficient	0.0115–0.0327
No. of unique data	1659
No. of observations	1354 ($F > 6\sigma$)
$R^* = \Sigma\|F_o - F_c\|/\Sigma F_o$	0.0434
$R^{**} = [\Sigma\omega(\|F_o - F_c\|)^2/\Sigma\omega\|F_o\|^2]^{1/2}$	0.0483

$-F_c)^2$. The largest peaks in the difference Fourier were osmium residuals of 3.04 and $-1.54\,e\,Å^{-3}$.

Tables of hydrogen atom coordinates, anisotropic thermal parameters, and a complete list of bond lengths and angles will be deposited at the Cambridge Crystallographic Data Centre.

4.4. H_2 binding thermodynamics

Three solutions for the internal competition for H_2 binding among $L_2OsXY(H)_2$ species were prepared by mixing equimolar $L_2OsX_2(H)_2$ and $L_2OsY_2(H)_2$ for the (X, Y) cases (Cl, Br), (Cl, I), and (Br, I). These establish halide redistribution equilibria to form some $L_2OsXY(H)_2$, within time of mixing. Integrations of ^1H and $^{31}P\{^1H\}$ NMR spectra of these three solutions under H_2 (with long pulse delay times) yield the results in Table 2.

4.5. Spectral data

4.5.1. $(P^iPr_3)_2OsBr_2H_4$

^1H (CD_2Cl_2/toluene-d_8 9:1, 20 °C): 2.93 (mult, 611), 1.34 (apparent q, $N = 6.5$, 36H), −10.63 (t, $J_{HP} = 10.1$, 4H). $^{31}P\{^1H\}$ (CD_2Cl_2, 21 °C): 10.6 (s).

4.5.2. $(P^iPr_3)_2OsI_2H_4$

^1H (CD_2Cl_2/toluene-d_8 9:1, 20 °C): 2.97 (mult, 6H), 1.30 (apparent q, $N = 7.0$, 36H), −10.63 (t, $J_{HP} = 10.0$, 4H). $^{31}P\{^1H\}$ (CD_2Cl_2, 21 °C): 10.6 (s).

4.5.3. $(P^iPr_3)_2OsClBrH_4$

$^{31}P\{^1H\}$ ($CDCl_3$, −21 °C): 21.9 (s).

4.5.4. $(P^iPr_3)_2OsClIH_4$

$^{31}P\{^1H\}$ ($CDCl_3$, −21 °C): 20.5 (s).

4.5.5. $(P^iPr_3)_2OsBrIH_4$

$^{31}P\{^1H\}$ ($CDCl_3$, −21 °C): 15.8 (s).

4.6. X-ray structure determination of $OsH_4Br_2(P^iPr_3)_2$

A small well-formed crystal was cleaved from a larger sample and affixed to the end of a glass fiber using silicone grease, and the mounted sample was then transferred to the goniostat where it was cooled to −174 °C for characterization (Table 6) and data collection ($6° < 2\theta < 55°$). A systematic search of a limited hemisphere of reciprocal space located a set of reflections with monoclinic symmetry and systematic absences corresponding to space group $P2_1$ or $P2_1/m$. Subsequent solution and refinement of the structure confirmed the non-centrosymmetric choice. Data were collected (Table 6) using a standard moving crystal–moving detector technique with fixed background counts at each extreme of the scan. Data were corrected for

Table 6
Crystallographic data for $OsH_4Br_2(P^iPr_3)_2$

formula = $OsBr_2P_2C_{18}H_{46}$	fw = 674.52 g mol^{-1}
$a = 8.783(2)$ Å	space group $P2_1$
$b = 15.305(3)$ Å	$T = -174$ °C
$c = 9.609(2)$ Å	$\lambda = 0.71069$ Å [a]
$\beta = 106.39(1)°$	$\rho_{calc} = 1.808$ g cm^{-3}
$V = 1239.30$ Å^3	$\mu = 84.7$ cm^{-1}
$Z = 2$	$R(F_o)$ [b] = 0.0614
No. of unique data 2951	$R_w(F_o)$ [c] = 0.0597
No. of observed data 2420	

[a] Graphite monochromator.
[b] $R = \Sigma||F_o|-|F_c||/\Sigma|F_o|$.
[c] $R_w = [\Sigma w(|F_o|-|F_c|)^2/\Sigma w|F_o|^2]^{1/2}$ where $w = 1/\sigma^2(|F_o|)$.

Lorentz and polarization terms and equivalent data averaged. An absorption correction was also applied, based on approximate indices for the faces of the fragment used. The structure was solved by direct methods (MULTAN78) and Fourier techniques. In spite of the absorption correction (transmission factors from 0.19 to 0.34), large residuals remained after refinement. In addition, several of the carbon atoms converged to non-positive definite thermal parameters. Since the residuals were not significantly lower with the anisotropic refinement, the final cycles allowed only the heavy atoms to vary anisotropically. Hydrogen atoms on carbons were placed in idealized calculated positions for the final cycles of refinement. Attempts to locate the hydrogen atoms bound to the metal were unsuccessful. A final difference Fourier was essentially featureless, the largest peak being $2.72\,e\,Å^{-3}$ at the Os site.

Tables of hydrogen atom coordinates, anisotropic thermal parameters, and a complete list of bond lengths and angles will be deposited at the Cambridge Crystallographic Data Centre.

Acknowledgements

This work was supported by the National Science Foundation. R.K. also thanks the NSF for a graduate fellowship.

References

[1] K.G. Caulton, *New J. Chem.*, *18* (1994) 25.
[2] J.T. Poulton, K. Folting, W.E. Streib and K.G. Caulton, *Inorg. Chem.*, *31* (1992) 3190.
[3] J.A.K. Howard, O. Johnson, T.F. Koetzle and J.L. Spencer, *Inorg. Chem.*, *26* (1987) 2930.
[4] D.G. Gusev, R. Kuhlman, G. Sini, O. Eisenstein and K.G. Caulton, *J. Am. Chem. Soc.*, *116* (1994) 2685.
[5] D.G. Gusev, V.F. Kuznetsov, I.L. Eremenko and H. Berke, *J. Am. Chem. Soc.*, *115* (1993) 5831.
[6] R. Kuhlman, D.G. Gusev, E. Clot, W.E. Streib, O. Eisenstein and K.G. Caulton, submitted to *J. Am. Chem. Soc.*

[7] M. Aracama, M.A. Esteruelas, F.J. Lahoz, J.A. Lopez, U. Meyer, L.A. Oro and H. Werner, *Inorg. Chem., 30* (1991) 288.
[8] D.G. Gusev, R. Kuhlman, J.R. Rambo, H. Berke, O. Eisenstein and K.G. Caulton, *J. Am. Chem. Soc., 117* (1995) 281.
[9] H.E. Bryndza, P.J. Domaille, R.A. Paciello and J.E. Bercaw, *Organometallics, 8* (1989) 8379.
[10] R. Kuhlman, W.E. Streib, J.C. Huffman and K.G. Caulton, *J. Am. Chem. Soc., 118* (1996) 6934.
[11] A. Albinati, V.I. Bakhmutov, K.G. Caulton, E. Clot, J. Eckert, O. Eisenstein, D.G. Gusev, V.V. Grushin, B.E. Hauger, W.T. Klooster, T.F. Koetzle, R.K. McMullan, T.J. O'Loughlin, M. Pélissier, J.S. Ricci, M.P. Sigalas and A.B. Vymenits, *J. Am. Chem. Soc., 115* (1993) 7300.
[12] D.W. Hart, R. Bau and T.F. Koetzle, *J. Am. Chem. Soc., 99* (1977) 7557.
[13] T.J. Johnson, A. Albinati, T.F. Koetzle, O. Eisenstein, J.C. Huffman and K.G. Caulton, *Inorg. Chem., 33* (1994) 4966.
[14] D.G. Hamilton and R.H. Crabtree, *J. Am. Chem. Soc., 110* (1988) 4126; P.J. Desrosiers, L. Cai, Z. Lin, R. Richards and J. Halpern, *J. Am. Chem. Soc., 113* (1991) 4173.
[15] J.S. Siegel and F.A.L. Anet, *J. Org. Chem., 53* (1988) 2629.